The Raman spectra of the different phases in the $CaSO_4$-H_2O system

Nagore Prieto-Taboada*, Olivia Gómez-Laserna, Irantzu Martínez-Arkarazo, María Ángeles Olazabal and Juan Manuel Madariaga

Department of Analytical Chemistry, University of the Basque Country, (UPV/EHU), Barrio Sarriena s/n, 48940, Leioa, Spain.
Email*: nagore.prieto@ehu.es, Tel.*: +34 94 601 82 94, Fax: +34 94 601 35 00

ABSTRACT

Although it is known that the $CaSO_4/H_2O$ system is formed by at least five different phases, this fact is not correctly documented in Raman spectroscopy studies. The main problem detected in the literature was the incorrect definition of the anhydrite, which produced the assignation of different spectra for a single compound. In this sense, two different spectra were clearly identified from the bibliography, which showed different main Raman bands at 1017 or 1025 cm^{-1}, although anhydrite could be present even as three different polymorphous species with different structures. A better knowledge of the whole system obtained from a review of the literature allowed new conclusions to be established. Thanks to that revision and the development of different thermodynamical experiments by Raman spectroscopy, the Raman spectra of each phase were successfully identified for the first time. In this way, the main Raman bands of gypsum-bassanite-anhydrite III-anhydrite II-anhydrite I were identified at 1008-1015-1025-1017-1017 cm^{-1} respectively. To conclude this work, the contradictions found in literature were critically summarized.

KEYWORDS: Raman spectroscopy, gypsum, insoluble anhydrite, soluble anhydrite, bassanite.

INTRODUCTION

The $CaSO_4$-H_2O system contains some of the most important compounds usually used in different fields nowadays and it includes three different minerals: gypsum ($CaSO_4 \cdot 2H_2O$), bassanite ($CaSO_4 \cdot 0.5H_2O$) and anhydrite ($CaSO_4$). Gypsum is the most abundant sulphate mineral in nature and it is widely used in many industry fields, such as construction, or as fertilizer. Calcium sulphate hemihydrate appears in nature as bassanite mineral and it is the most-produced inorganic compound in the world, being known as "Plaster of Paris". Lastly, anhydrite is frequently found in evaporate deposits together with gypsum and it also has high importance in industry[1-3]. In spite of its relevance, there are many unknown points in the hydration-dehydration process of the $CaSO_4$-H_2O system because it has demonstrated to be a really complex system, which is affected by numerous factors such as impurities, temperature, pressure, humidity, etc[4, 5]. In order to solve these unknowns points, a large number of studies about this system carried out by many different techniques as, for example, Raman spectroscopy, x-ray diffraction (XRD) or thermo gravimetric analysis (TGA)[5-9] can be taken into account. However, there still seems to be many unanswered questions about the system[2, 7].

Raman spectroscopy is one of the most used techniques for the study of these kind of systems due to its high sensitivity to small structure variations, which allows polymorphic compounds to be distinguished[10-13]. Furthermore, when hydration-dehydration processes are studied, it is very useful to carry out the monitoring of the loss of water in order to try to determine the transition point between different phases and this technique can also be used to obtain this information through the study of the 2900-3700 cm^{-1} region[6, 7, 14, 15].

Nevertheless, at the same time, it is remarkable the numerous different Raman spectra collected in bibliography for the different phases of $CaSO_4$-H_2O, which are reported by different authors without a clear consensus, being the main problems related to bassanite and anhydrite phases [1, 6, 7, 10, 14, 16-21]. These incongruences go beyond the natural evolution of the research in this field because they are still present in the latest works which could lead to difficulties for new researches. For that reason, this work aims to clarify once and for all, the Raman spectra of the different phases of $CaSO_4$-H_2O, firstly by a thorough study of the bibliography and a subsequent complementation with the required experimental work.

$CaSO_4$-H_2O system and problems detected in Raman spectroscopy studies

Apart from the natural development of the research that could generate the finding of incorrect information in older articles, the most important problem encountered in bibliography is related to the description of the different phases of $CaSO_4$-H_2O. In general, only three phases are defined: gypsum ($CaSO_4 \cdot 2H_2O$), bassanite ($CaSO_4 \cdot 0.5H_2O$) and anhydrite ($CaSO_4$), which match with the minerals found in nature. However, the complete hydration-dehydration system includes more than one type of anhydrite and this fact was the key to understand the contradictions found in literature to obtain the correct Raman spectra of each phase.

A summary of the studied system formed by at least five different phases is collected in Table 1. The starting point is gypsum which is the most common phase and it dehydrates to form calcium sulphates with lower H_2O content, being some of them metastable phases, as bassanite and anhydrite III (AIII). The first dehydrated phase formed is known as bassanite or hemihydrate and it could be present in different morphologic forms (α, β or β'), depending on the dehydration process. Heating gypsum in wet conditions produces α form, whereas heating

it under ambient conditions results in the formation of the β type hemihydrate [2, 3, 8]. It is necessary to mention that although this compound is a well-known intermediate phase of the system, sometimes it is not observed, as its formation depends on the heating conditions. Continuing with the dehydration process, above temperatures close to 110 °C, the hemihydrate forms AIII, also called soluble anhydrite or γ-$CaSO_4$ (analogously to hemihydrate, this compound could present α or β modifications)[8]. At approximately 300 °C it is formed the insoluble anhydrite (also called β-$CaSO_4$ or anhydrite II (AII)), corresponding to the mineralogical form of anhydrite, whose rehydration is very low or even null depending on the temperature reached. Finally, there also exists a high temperature variety of anhydrite called anhydrite I (AI) or α-$CaSO_4$, which is stable above 1180°C[2-4, 8, 9, 22, 23].

The inner complexity of the system could be the reason for some of the incongruences found in literature and, besides, its understanding results also complicated by the variability of nomenclatures used for these compounds, which usually depend on the research fields. Another difficulty is related to the transition temperature ranges, which are different depending on many factors and change among authors[4, 5]. This fact complicates the determination of the phases by the temperature and another control parameter, such as the water loss, becomes necessary to differentiate between them. Moreover, the lack of water only indicates the presence of an anhydrous compound but this system is formed by at least three anhydrous phases. Therefore, the assignment of the obtained spectrum, by monitoring of the water loss, could be incorrect if this point is not taken into account. In fact, that is the main problem detected in the literature. Then, although Raman spectroscopy is one of the most useful techniques to carry out this work, the correct understanding of the whole system is crucial.

Raman spectra of $CaSO_4$-H_2O system in the literature

The spectrum of gypsum was the most clearly determined and it was collected in many articles as well as in renowned databases. The different bands collected in the bibliography are summarized in Table 2. Gypsum was the less problematic compound because its stability allows the measurement of standards, being the deviation of the main Raman band from 1008 cm^{-1} observed in some articles, generally related to the resolution of different equipment, the only remarkable point.

In the case of $CaSO_4 \cdot 0.5H_2O$, more discrepancies were found owing to the difficulty of isolating the spectrum in thermodynamic studies because it is a metastable compound. Besides, it is known that this compound could be not observed in the heating process and it could be confusing to determine the phase of the system observed[5]. Even so, bassanite is also found as mineral and it was measured as a standard, identifying the main Raman band of this compound centred at 1015 cm^{-1}, as can be seen in Table 3.

Finally, the more difficult and, therefore, more erroneously identified in the literature, was the case of the anhydrite spectrum. As it has been previously mentioned, three anhydrite polymorphs form the $CaSO_4$-H_2O system, however, this fact was not commonly found in the bibliography, so the determination of the anhydrite spectrum was extremely confusing. Considering the information described in the literature, the main incongruence was the clear identification of two spectra related to anhydrite, with the main Raman bands at 1017 and 1025 cm^{-1}, as can be observed in Table 4.

After a thorough study of the data found in the bibliography, it was possible to state that the spectrum with the band at 1025 cm^{-1} was always associated to thermodynamic studies. This spectrum was identified at approximately 110ºC as a consequence of gypsum heating and it was related to the total absence of water. Knowing the $CaSO_4$-H_2O system, the anhydrite form present at that temperature was the metastable soluble anhydrite (AIII). This compound is very difficult to isolate because it is rather unstable and its rehydration is very fast as it was described in the literature [6, 7, 10]. On the other hand, the spectrum with the main Raman band at 1017 cm^{-1} was always related to the natural anhydrite by the direct measurement of minerals or standards (not thermodynamic studies). Regarding that, this spectrum corresponded to the insoluble anhydrite or AII[14, 16, 18]. For that reason, in studies of archaeology, anhydrite is usually identified by its main Raman band at 1017 cm^{-1}, which belongs to the natural anhydrite and the band at 1025 cm^{-1} has been referenced as other compounds[24-26], which sometimes could be erroneous.

Another important difference between these spectra, in addition to the shift of the main Raman band, was the appearance of a new band at 608 cm^{-1} in the case of insoluble anhydrite spectrum, which was related to the ν_4 (SO_4) flexion vibration due to differences of their structures (AII rhombic and AIII hexagonal).

In the whole, the hypothesis obtained from the bibliography review concluded that, the two spectra collected in the literature belong to two different anhydrites with different structures (not the same anhydrite). This hypothesis could mean an important advance in the determination of the spectra of the $CaSO_4$-H_2O system and, thus, it is necessary to confirm it, as well as to complete the system identification with the spectrum of the anhydrite AI, which was not found in the literature.

EXPERIMENTAL

Materials and Methods

In order to confirm the hypothesis obtained from the literature revision, a thermodynamic study of the system was carried out. For this purpose, a gypsum standard (Fluka Analytical, Sigma Aldrich, USA) was measured by Raman spectroscopy at three different temperature programs.

The first one consisted of an increment of 0.5ºC·min^{-1} up to 350ºC, to obtain the AIII compound and followed by the monitoring of the cooling process at the same temperature variation to confirm its rehydration capacity. In this process, spectra were collected every 2ºC. The second temperature program was based on a faster increment of temperature (25ºC·min^{-1}) up to 600ºC and followed by a slower temperature ramp (10ºC·min^{-1}) up to 800ºC to obtain the AII compound. In this case, the cooling process was also monitored (at the same temperature ramp) to check the null rehydration capacity of this compound. In this way, spectra were collected only in the second ramp every 20ºC.

Finally, the temperature of the AI transition is well-known and, therefore, it was possible to obtain it from the heating of gypsum at 1300ºC, hence, the last temperature program involved a fast heating of the gypsum at 250ºC·min^{-1}up to 1300ºC, collecting the spectrum once this temperature was reached.

To confirm the AII spectrum, its synthesis was carried out in an electric oven by heating gypsum at 600ºC and then measuring its Raman spectrum. The resulting compound was also

measured during 22 days in order to confirm its null rehydration process under room conditions and after 6 days mixed with water.

It is necessary to remark that all products were obtained under atmospheric pressure so, only β-modifications of bassanite and AIII were studied, which was close to technical conditions during cement milling.

Instrumentation

A Renishaw InVia confocal microRaman spectrometer was used for the thermodynamic study. This spectrometer is coupled to a DMLM Leica microscope (UK) focused through a 50x lens (N PLAN EPI, 0.40 aperture, 1.1 mm working distance) and it uses a 514 nm laser as excitation source (the nominal laser power settings at the surface of the samples were 20 mW) in order to minimize the black body effect as a result of measuring at high temperatures. The used grating was 1800 lines/mm, the spectra were acquired in synchro scan acquisition mode, the data were not calibrated in intensity terms but the spectral axis was calibrated with elemental silicon measuring its main Raman bands at 520 cm^{-1}.Finally, a CCD detector (Peltier cooled) and the Wire 3.3 software (Renishaw, UK) were used for the detection and data collections, respectively. The microscope comprises a Prior Scientific motorised XYZ stage system with a joystick and it is equipped with a TV microcamera. The spectrometer was coupled to a high temperature stage TS1500 Linkam Scientific Instrument (UK) for the automatic control of the measurement temperature. The sample was placed inside a ceramic sample cup, homogeneously heated from room temperature up to 1500ºC, if necessary, and controlled by the Wire 3.3 software. Spectra were taken at a resolution of 1 cm^{-1}, during 15 s, 1 accumulation and 100% laser power in two ranges: 100-3800 cm^{-1} to observe the H_2O content evolution (only in the first temperature program) and 100-1500 cm^{-1}.

In order to confirm the phases, taking into account the complexity of the system, all the thermodynamic studies were carried out analogously by powder X-ray diffraction (XRD) using a Bruker diffractometer (model D8 Advanced) operating at 20 mA and 30 kV, and equipped with a Cu tube, a Vantec-1 PSD detector, and an Anton Parr HTK2000 high-temperature furnace. The powder standards were recorded in 2θ steps of 0.033º in the $10 \leq 2\theta \leq 80$ range, counting for 1 s per step, without delay time.

On the other hand, an I-Raman-532S ultramobile Raman spectrometer (B&WTEK^{INC}, Newark, USA) was used for the daily measurements and to study the stability of the gypsum under the laser power. It was supplied with a probe head that can be coupled with long-range lenses, focusing with magnifications of 50x, and connected to a micro camera. The excitation wavelength was 532 nm (the nominal laser power settings at the surface of the samples were 33 mW) and the dispersed Raman signals were measured by a Peltier cooled CCD detector. The spectra were collected in the wavenumber range of 62-3750 cm^{-1} (non changeable) with a spectral resolution of 5 cm^{-1}. Data acquisition was carried out by the BWSpec4.02_15 software package and the analysis of the results was undertaken by the Omnic 7.2 software (Nicolet).

Additionally, to study the stability of the samples under the laser power, an innoRaman ultramobile Raman spectrometer (B&WTEK^{INC}, Newark, USA) was used. Both ultramobile spectrometers have practically the same features, being the main difference between both equipments the excitation wavelength. In this case, it was 785 nm (the nominal laser power settings at the surface of the samples was 255 mW). The spectra were collected in the

wavenumber range of 100-3000 cm^{-1} (non changeable) with a spectral resolution of 3.5 cm^{-1}. Data acquisition was carried out by the BWSpec3.26 software package.

Finally, the different spectra of the literature were compared with our previous results collected in the e-visnich, e-visart and e-visarch dispersive Raman, as well as other FT-Raman spectral databases reported in the literature[20, 27-29].

RESULTS AND DISCUSSION

Raman spectra of the different phases of the $CaSO_4$-H_2O system

The first temperature program carried out allowed detailed information to be collected from the heating process. Apart from the gypsum spectrum, in addition, two different spectra were distinguished, as can be seen in Figure 1. The first one was observed up to 110ºC with the main Raman band centred at 1014 cm^{-1} and identified as bassanite. In the heating process, this compound could not be completely isolated because of the presence of a mixture of phases which can be easily observed by a deconvolution of the main Raman band (see Figure 1). However, its identification was possible thanks to the shift of the main Raman band, the temperature control and the monitoring of the water presence. In this sense, this compound has 0.5 molecules of water and therefore, it was identified by the band at 3550 cm^{-1}, which was related to the water presence. At 110ºC, the main Raman band was suddenly shifted to 1025 cm^{-1} and the formation of the soluble anhydrite (AIII) was confirmed by the complete disappearance of water signal. Moreover, apart from the main Raman band, which is the most evident change and as can be seen in Table 5, the bands in the range of 400-700 cm^{-1} and 110-1200 cm^{-1} also present shifts in their position.

The monitoring of the water bands intensity versus time revealed the graphic collected in Figure 2a, in which different dehydration phases could be distinguished thanks to the differences among the slopes. The intersection between lines revealed the transition point of the dehydrated compounds formed in the process. The first one, at approximately 57ºC, was related to the gypsum-bassanite transition when bassanite started to coexist together with gypsum. Then, bassanite predominated up to approximately 115ºC. At that point, the dehydration processes was complete and soluble anhydrite was the main compound of the system.

This effect is also observed in Figure 2b, in which the evolution of bassanite is associated with the disappearing of gypsum whereas the soluble anhydrite formation involves the consumption of bassanite.

The cooling process of this temperature program indicated a rehydration of the formed soluble anhydrite to form again bassanite. This fact confirmed once more the identification of the soluble anhydrite, which could be rehydrated in contrast with the insoluble anhydrite, whose rehydration is very low or null.

Owing to the effect of the black body radiation, the increment of temperature generated the growth of the baseline and, therefore, it caused more difficulties in the identification of the compounds and it could even mask completely the spectra. This effect was increased when the heating was slow because of the effect in the whole system (not only the sample) which emits also some radiation that can reach the detector. However, when the heating processes were carried out faster, this effect could be slightly minimized allowing to study a range of temperatures enough for identifying the main Raman bands of the first two anhydrites. Taking this into account, for the identification of the remainder anhydrites the heating temperature velocity of the programs was increased. Thanks to that, in the second temperature program,

the identification of the insoluble anhydrite was possible by the observation of its main Raman band at 1017 cm^{-1}. Furthermore, the rehydration of this compound was not observed in the cooling process, confirming once again the identification of AII anhydrite.

Finally, the spectrum of the AI anhydrite was obtained for the first time in the bibliography by a heating process at 1300ºC. As can be seen in Figure 3, the difference between the spectrum of the AII and AI anhydrites was the identification of two new Raman bands at 969 and 170 cm^{-1}, which are the consequence of the different crystallographic structures, as well as, low movements in some of the less intense bands, as can be observed in Table 5. Besides, differences between relative intensities of the bands were observed and collected in Table 6. It is necessary to mention that these new bands cannot be attributed either to CaO because it is inactive in Raman spectroscopy[30], or to SO_3 or SO_4^{2-}[31-33].

Confirmation of the obtained spectra

Apart from the automatic heating programs through temperature cell, the synthesis of the insoluble anhydrite was carried out in an electric oven to obtain the complete spectra of this compound as well as to monitoring its rehydration under room conditions. This monitoring was carried out not only by the control of the main Raman band, but also, by the control of the width of this band by deconvolution analysis in order to discard a mixture of compounds. As it was expected, no rehydration was observed. In addition, in order to force the hydration of this compound, its mixture with water was monitored too. In this case, it was possible to observe a little rehydration according to the possibilities of this anhydrite heated to 600ºC. All of these results showed again that the studied compound with the main Raman band at 1017 cm^{-1} was the insoluble anhydrite.

On the whole, thanks to this study, the Raman spectra of all the $CaSO_4$-H_2O system were obtained and its main Raman features are summarized in Table 5.

It should be mentioned that small differences between the Raman bands positions for the same compound that could be found in bibliography are generally related to equipment variables as the instrument resolution. The shifts of the main Raman band could generate the wrong identification of compounds. For that reason, it is strongly recommended to reference the main Raman bands of these compounds to the gypsum main Raman band, measured at the same conditions. Taking into account that, this gypsum band is clearly defined at 1008 cm^{-1}, it could act like a standard in order to avoid the mentioned instrumental effect.

In addition, when metastable compounds are present differences between the main Raman bands positions could also appear, because of the mixture of phases. For that reason, the deconvolution of the main Raman band is also recommended to solve the ambiguity that it could generate.

Taking into account the complexity of the system and in order to avoid any doubt in the identification of the different phases, apart from the Raman measurements, a XRD analysis was carried out. In this way, as can be seen in the Figure 4, four different phases were clearly observed, corresponding to gypsum, AIII, AII and AI formed at similar temperature transitions to those obtained in the Raman spectroscopy thermodynamical studies. In the case of bassanite, due to the similarities in the XRD spectra, the mixture of compounds and the small temperature range in which it appears, its presence was not so evident. However, a study in depth of the obtained spectra allows its presence to be confirmed. Thus, the same

results obtained by Raman spectroscopy were achieved corroborating definitively the different measured phases.

Stability of the system under laser radiation

From our previous studies, the transformation of gypsum into soluble anhydrite was observed in mortars rich in iron oxides, probably as a consequence of the laser radiation. To clarify the stability of gypsum under laser radiation, different tests were carried out.

In this way, a gypsum standard was exposed to a high laser radiation at 785 nm (33 mW of power) during a long exposing time (more than 15 minutes) without obtaining any changes, either in the main Raman band position or in the width of the band. Moreover, in order to generate an aggressive environment that could absorb heat, gypsum was applied as a thin layer on an iron piece. Again, the laser radiation was not enough for the phase transition. For that reason, the same test was carried out with a more powerful laser that provided 255 mW of power in the surface of the sample. In this case either, the long irradiation time was not enough for changing the main Raman band of the gypsum.

Taking into account all these results, as well as the effect observed in real samples, the generation of micro-conditions in the sample was supposed. Therefore, it could conclude that the stability of gypsum under the laser seemed to be influenced by the matrix and owing to this, soluble anhydrite could be erroneously identified. For that reason, the control of the laser power is recommended above all in this kind of matrix.

CONCLUSIONS

The contradictions found in the bibliography can be associated with an incomplete or incorrect definition of the system. In the case of gypsum, the spectrum was clearly defined in

the literature. However, for bassanite, the differences found were related to its metastable character, which generates differences in the main Raman band, due to the transition processes, which is easily detectable by the deconvolution of the bands.

Nevertheless, the main problem in the understanding of the system was connected to anhydrite, whose main Raman band was defined in the literature at 1017 or 1025 cm^{-1}, depending on the authors. This incongruence was consequence of the different polymorphic anhydrites of the $CaSO_4$-H_2O system (AI, AII and AIII). In this way, the main Raman band at 1017 cm^{-1}, it was always related to AII or natural anhydrite. In contrast, the Raman band at 1025 cm^{-1} was characterised in the thermal studies as it is a metastable compound known as AIII or soluble anhydrite. Worth noting that, these first phases were sensitive to phase transformation by laser power, depending on the studied matrix. Finally, AI showed the main Raman band at 1017 cm^{-1} and thereby, this work completes the spectra of the whole system and could be the starting point to finish with the contradictions found in the bibliography.

Acknowledgements

This work has been financially supported by the project PRIACE (ref: CTM2012-36612) from the Spanish Ministry of Economy and Competitiveness (MINECO). N. Prieto-Taboada and O. Gómez-Laserna acknowledge their grants from the University of the Basque Country. Technical and human support provided the Raman-LASPEA and X-Ray diffraction laboratories by SGIker (UPV/EHU, MICINN, GV/EJ, ERDF and ESF) are also gratefully acknowledged.

BIBLIOGRAPHY

(1) Wang, Y.; Kim, Y.; Christenson, H. K.; Meldrum, F. C. *Chem.Commun.* **2012**, *48*, 504-506.

(2) Charola, A.; Pühringer, J.; Steiger, M. *Environ.Geol.* **2007**, *52*, 339-352.

(3) Freyer, D.; Voigt, W. *Mon.Chem.* **2003**, *134*, 693-719.

(4) Christensen, A. N.; Olesen, M.; Cerenius, Y.; Jensen, T. R. *Chem.Mater.* **2008**, *20*, 2124-2132.

(5) Lou, W.; Guan, B.; Wu, Z. *J.Therm.Anal.Calorim.* **2011**, *104*, 661-669.

(6) Chang, H.; Jane Huang, P.; Hou, S. C. *Mater.Chem.Phys.* **1999**, *58*, 12-19.

(7) Prasad, P. S. R.; Pradhan, A.; Gowd, T. N. *Curr.Sci.* **2001**, *80*, 1203-1207.

(8) Seufert, S.; Hesse, C.; Goetz-Neunhoeffer, F.; Neubauer, J. *Cem.Concr.Res.* **2009**, *39*, 936-941.

(9) Bezou, C.; Nonat, A.; Mutin, J. -.; Christensen, A. N.; Lehmann, M. S. *J.Solid State Chem.* **1995**, *117*, 165-176.

(10) Chio, C. H.; Sharma, S. K.; Muenow, D. W. *Am.Mineral.* **2004**, *89*, 390-395.

(11) Colomban, P. *J.Raman Spectrosc.* **2012**, *43*, 1529-1535.

(12) Gómez-Laserna, O.; Olazabal, M. A.; Morillas, H.; Prieto-Taboada, N.; Martínez-Arkarazo, I.; Arana, G.; Madariaga, J. M. *J.Raman Spectrosc.* **2013**, *44*, 1277-1284.

(13) Das, R. S.; Agrawal, Y. K. *Vib.Spectrosc.* **2011**, *57*, 163-176.

(14) Buzgar, N.; Buzatu, A.; Sanislav, I. V. *Analele Ştiintifice ale Universităţii "Al.I.Cuza" din Iaşi.* **2009**, *55*, 5-23.

(15) Đuričković, I.; Claverie, R.; Bourson, P.; Marchetti, M.; Chassot, J.; Fontana, M. D. *J.Raman Spectrosc.* **2011**, *42*, 1408-1412.

(16) Liu, C.; Zheng, H. *Chinese Phys.Lett.* **2012**, *29*, 049101.

(17) Sarma, L. P.; Prasad, P. S. R.; Ravikumar, N. *J.Raman Spectrosc.* **1998**, *29*, 851-856.

(18) Liu, Y.; Wang, A.; Freeman, J. J. *40th Lunar and Planetary Science Conference.* **2009**, *abstract 2128.*

(19) Brotton, S. J.; Kaiser, R. I. *J.Phys.Chem.Lett.* **2013**, *4*, 669-673.

(20) Downs, R. T. *Program and Abstracts of the 19th General Meeting of the International Mineralogical Association in Kobe, Japan*; 2006; pp O03-13.

(21) Douthwaite, R. and Yarwood, J. D.,Simon. *Spectroscopic Properties of Inorganic and Organometallic Compounds Vol.40,* 1st Edition ed.; Royal Society of Chemistry:UK; 2009.

(22) Kontogeorgos, D. A.; Founti, M. A. *Thermochim.Acta.* **2012**, *529*, 6-13.

(23) Singh, N. B.; Middendorf, B. *Prog.Cryst.Growth Charact.Mat.* **2007**, *53*, 57-77.

(24) Prieto-Taboada, N.; Maguregui, M.; Martinez-Arkarazo, I.; Olazabal, M.; Arana, G.; Madariaga, J. M. *Anal.Bioanal.Chem.* **2010**, *399*, 2949-2959.

(25) Tournié, A.; Prinsloo, L. C.; Paris, C.; Colomban, P.; Smith, B. *J.Raman Spectrosc.* **2011**, *42*, 399-406.

(26) Aliatis, I.; Bersani, D.; Campani, E.; Casoli, A.; Lottici, P. P.; Mantovan, S.; Marino, I. *J.Raman Spectrosc.* **2010**, *41*, 1537-1542.

(27) Maguregui, M.; Prieto-Taboada, N.; Trebolazabala, J.; Goienaga, N.; Arrieta, N.; Aramendia, J.; Gómez-Nubla, L.; Sarmiento, A.; Olivares, M.; Carrero, J. A.; Martínez-Arkarazo, I.; Castro, K.; Arana, G.; Olazabal, M. A.; Fernández, L. Á.; Madariaga, J. M. *1st International Congress of Chemistry for Cultural Heritage (ChemCH).* **2010**, 168-168.

(28) Castro, K.; Pérez-Alonso, M.; Rodríguez-Laso, M. D.; Fernández, L. Á.; Madariaga, J. M. *Anal.Bioanal.Chem.* **2005**, *382*, 248-258.

(29) Pérez-Alonso, M.; Castro, K.; Madariaga, J. M. *Curr.Anal.Chem.* **2006**, *2*, 89-100.

(30) Dubina, E.; Korat, L.; Black, L.; Strupi-Šuput, J.; Plank, J. *Spectrochim.Acta A.* **2013**, *111*, 299-303.

(31) Chrysostom, E. T. H.; Vulpanovici, N.; Masiello, T.; Barber, J.; Nibler, J. W.; Weber, A.; Maki, A.; Blake, T. A. *J.Mol.Spectrosc.* **2001**, *210*, 233-239.

(32) Tang, S.; Brown, C. W. *J.Raman Spectrosc.* **1975**, *3*, 387-390.

(33) Vargas Jentzsch, P.; Kampe, B.; Ciobotă, V.; Rösch, P.; Popp, J. *Spectrochim.Acta A.* **2013**, *115*, 697-708.

(34) Sarmiento, A.; Maguregui, M.; Martínez-Arkarazo, I.; Angulo, M.; Castro, K.; Olazábal, M. A.; Fernández, L. Á.; Rodríguez-Laso, M. D.; Mujika, A. M.; Gómez, J.; Madariaga, J. M. *J.Raman Spectrosc.* **2008**, *39*, 1042-1049.

(35) Castro, K.; Sarmiento, A.; Maguregui, M.; Martínez-Arkarazo, I.; Etxebarria, N.; Angulo, M.; Barrutia, M.; González-Cembellín, J.; Madariaga, J. *Anal.Bioanal.Chem.* **2008**, *392*, 755-763.

(36) Prieto-Taboada, N., Gómez-Laserna, O., Ibarrondo, I., Martinez-Arkarazo, I., Olazabal, M. A. and Madariaga, J. M. In *Conference on Micro-Raman and Luminiscence Studies in the earth and planetary sciences (CORALS II)* Lunar and Planetary Institute; Lunar and Planetary Institute (LPI) y Consejo Superior de Investigaciones Científicas (CSIC):Houston, 2011; pp 66-67.

(37) Paluszkiewicz, C.; Czechowska, J.; Ślósarczyk, A.; Paszkiewicz, Z. *J.Mol.Struct.* **2013**, *1034*, 289-295.

(38) Aramendia, J.; Gomez-Nubla, L.; Arrizabalaga, I.; Prieto-Taboada, N.; Castro, K.; Madariaga, J. M. *Corros.Sci.* **2013**, *76*, 154-162.

(39) Morillas, H.; Maguregui, M.; Gómez-Laserna, O.; Trebolazabala, J.; Madariaga, J. M. *J.Raman Spectrosc.* **2013**, *44*, 1700-1710.

(40) Veneranda, M.; Irazola, M.; Pitarch, A.; Olivares, M.; Iturregui, A.; Castro, K.; Madariaga, J. M. *J.Raman Spectrosc.* **2014**, *45*, 228-237.

(41) Makreski, P.; Jovanovski, G.; Dimitrovska, S. *Vib.Spectrosc.* **2005**, *39*, 229-239.

(42) Prieto-Taboada, N.; Ibarrondo, I.; Gómez-Laserna, O.; Martinez-Arkarazo, I.; Olazabal, M. A.; Madariaga, J. M. *J.Hazard.Mater.* **2013**, *248-249*, 451-460.

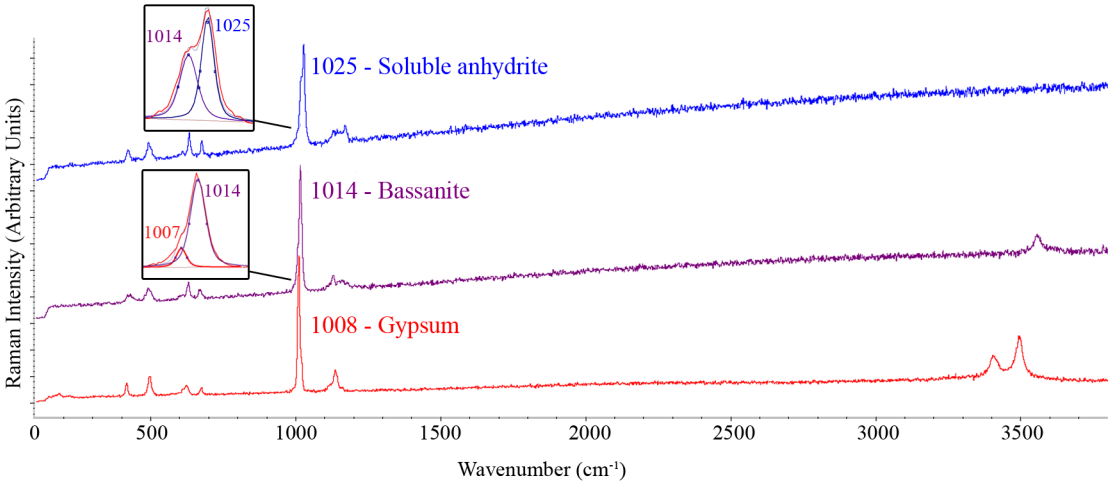

Figure 1.- The three spectra differentiated in the first heating program of gypsum (up to 350ºC) in which it was possible to identify the soluble anhydrite with the main Raman band at 1025 cm^{-1}, as well as the mix of compounds thanks to the deconvolution analysis.

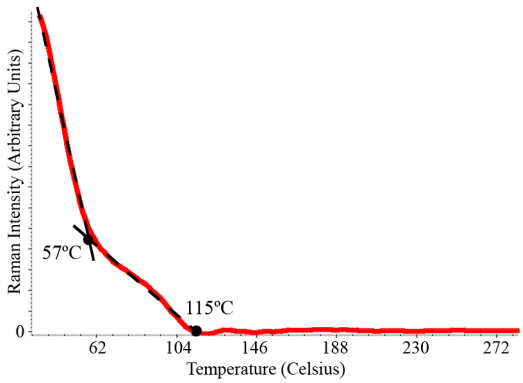

Figure 2.- Graphical representation of the intensity of the Raman bands of water along the heating process, which indicates two dehydration phases related with the bassanite (57ºC) and soluble anhydrite formation (115ºC).

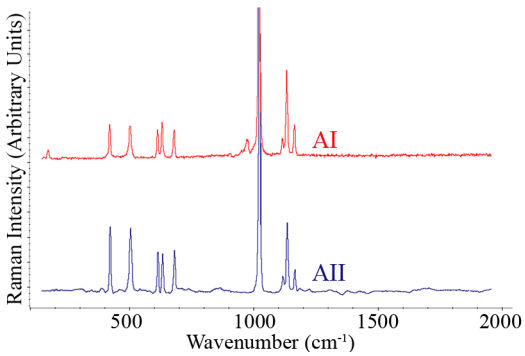

Figure 3.- Raman spectra of AII and AI in which two new bands at 969 and 170 cm^{-1} are present (due to the differences in the crystallization of AI anhydrite). Differences between relative intensities of the bands are also observed.

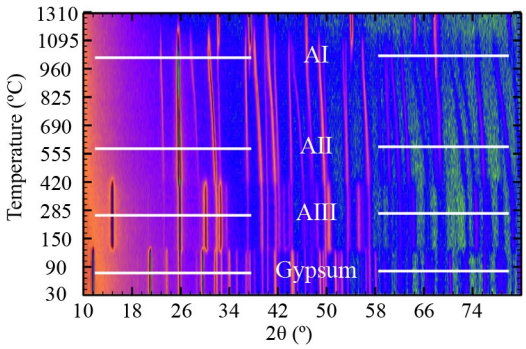

Figure 4.- Evolution of the XRD spectra in which it is possible to observe easily gypsum, AIII, AII and AI phases.

Table 1.- Summary of the different phases of the hydration-dehydration system of $CaSO_4$-H_2O.

Common name	**Gypsum**	**Bassanite**	**Anhydrite III**	**Anhydrite II**	**Anhydrite I**
Formula	$CaSO_4 \cdot H_2O$	$CaSO_4 \cdot 0.5H_2O$	$CaSO_4$		
Structure	Monoclinic	Monoclinic/Rhombohedric	Hexagonal	Orthorhombic	Cubic
Relative transition temperature	-	>45-110 ºC	110-300ºC	300-1180ºC	>1180ºC
Thermodynamic stability	Stable	Metastable	Metastable	Stable	Stable
Other names		Hemihydrate, α,β-$CaSO_4 \cdot 0.5H_2O$, Plaster of Paris	Soluble anhydrite, γ-$CaSO_4$	Insoluble, anhydrite, dead gypsum, β-$CaSO_4$, natural anhydrite	α-$CaSO_4$

Table 2.- Raman bands for gypsum $CaSO_4 \cdot 2H_2O$ in cm^{-1}.

References	ν_2 (SO_4)		ν_4 (SO_4)		ν_1 (SO_4)	ν_3 (SO_4)
[27-29]	414	493	619	670	1008	1135
[20]	414	492	619	670	1008	1140
[6]	416	492	622	672	1010	1138
[14]	415	494	620	671	1008	1136
[34]	413	492	619	673	1008	1132
[35]	413	492	620	671	1008	1135
[36]	413	492	619	673	1008	1132
[12]	414	493	619	670	1008	1135

Table 3.- Raman bands for bassanite $CaSO_4 \cdot 0.5H_2O$ in cm^{-1}.

References	ν_2 (SO_4)		ν_4 (SO_4)		ν_1 (SO_4)	ν_3 (SO_4)	
[27-29]	430	487	628	668	1015	1128	1148
[18]	427	487	628	668	1015	1128	-
[37]	428	490	625	667	1015	1130	1170
[38]	424	487	628	668	1015	-	-
[39]	429	487	627	668	1015	1128	-
[40]	-	-	-	-	1015	-	-

Table 4.- Raman bands for anhydrite $CaSO_4$ in cm^{-1} where two different spectra could be distinguished.

References	ν_2 (SO_4)		ν_4 (SO_4)			ν_1 (SO_4)	ν_3 (SO_4)		
[27-29]	417	499	609	628	676	1017	1112	1129	1160
[20]	417	499	610	628	676	1017	1111	1129	1159
[34]	417	500	609	627	675	1017	1112	1130	1160
[41]	415	498	609	627	676	1017	1111	1128	1159
[24]	417	500	609	627	675	1017	-	1130	1160
[42]	417	500	609	627	675	1017	-	(1132)	(1160)
[39]	417	500	609	627	675	1017	1112	1130	1160
[16]	416	498	608	627	675	1017	1110	1128	1159
[27-29]	422	491	-	630	673	1025	-	-	1165
[6]	423	493	-	630	672	1024	-	1120	1166
[7]	424	490	608	628	668	1026	1105	1152	1174

Table 5.-Suggested Raman spectra of all the compounds in the $CaSO_4$-H_2O system obtained in this study.

Compound	*	**ν_2 (SO_4)**		**ν_4 (SO_4)**			*	**ν_1(SO_4)**	**ν_3 (SO_4)**			**(H_2O)**	
Gypsum	-	415	495	-	620	673	-	1008	-	1134	-	3401	3491
Bassanite	-	428	489	-	627	669	-	1015	-	1128	-	-	3553
AIII	-	420	490	-	630	673	-	1025	-	-	1167	-	-
AII	-	417	499	609	628	675	-	1017	1111	1128	1160	-	-
AI	170	417	497	609	628	676	969	1017	1108	1127	1158	-	-

*The vibrational attribution of these new bands must be studied deeply.

Table 6.- Relative intensities of the Raman bands at 400-700 cm^{-1} with respect to the main Raman band at 1017 cm^{-1} for anhydrites AI and AII.

AII		**AI**	
Raman band	**Relative intensity**	**Raman band**	**Relative intensity**
417	0.21	417	0.12
499	0.20	497	0.11
609	0.13	609	0.10
628	0.12	628	0.12
675	0.13	676	0.10

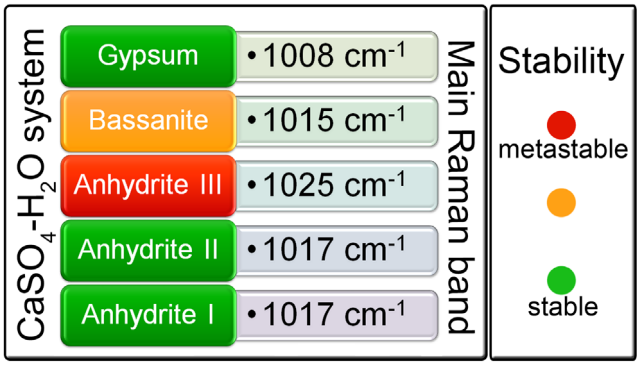

Figure 5.-“for TOC only”